Rock Mech. Rock Engng. (1995) 28 (3), 145–165

Rock Mechanics and Rock Engineering

Numerical Model for Rock Bolts with Consideration of Rock Joint Movements

By

M. Marenče[1] and **G. Swoboda**[2]

[1]Geomechatronic Center Linz, Hagenberg i.M., Austria
[2]University of Innsbruck, Innsbruck, Austria

Summary

The stability of any underground structure during and after excavation is the most important question for designers, because any kind of collapse may destroy large parts of a finished tunnel, causing major repairs and time loss. Preliminary calculations are therefore of great importance. A calculation is only useful, however, when the underlying numerical model correctly describes natural behaviour. The rock bolts used in tunnel excavations are mostly untensioned grouted bolts, and this type of bolt is the main focus of this work. From the model of the grouted bolt, other types of rock bolts can also be modelled by the theory presented herein. Bolt behaviour in intact rock mass is so different from behaviour when a bolt intersects a joint, that a model with two different elements is suggested for a numerical calculation; one element for the bolt in the rock mass and one as a bolt intersecting with a joint.

The model for both elements is verified by the experimental results. The numerical results correspond favourably with the experimental work. A variation of the parameters important for the behaviour of the bolt in intersection with the joint is shown. As an implementation of the bolt model, the numerical simulation of excavation and stabilisation of one road tunnel is presented.

1. Introduction

Rock bolts, in combination with a shotcrete lining, are the most important support elements and are widely used. The reason for using rock bolts is their ease of transportation, storage and installation, and also their superior reinforcement effect. The effect of the bearing capacity of rock bolts is very well known from experiments and "in situ" tests, but modelling of this effect is complicated because of a complex interaction between the bolt and the rock. The effect can be considered as an additional support load, as acting on the excavation boundary, as an increase of the stiffness and strength of the rock mass, and as a local support element to prevent the falling down or loosening of rock blocks.

The reinforcement effect of rock bolts depends not only on this axial and shear resistance, but also on the rock mass. In the continuous rock mass, rock bolts act

mostly with their axial resistance. In the jointed rock mass the shear resistance of the bolt also becomes important at the place where the bolt intersects the joint. While the axial resistance acts in approximately the same way for all rock bolt types, the shear resistance is important only for bolts with a continuous contact between the rock mass and the bar, as grouted and frictional bolts. The modelling of axial and shear resistances are so different that they are very often considered as separate problems in the literature on the subject.

The continuous rock mass supposes either the rock masses to be without cracks or that the inhomogeneities, as joints and schistosity, are considered by efficiently diminished rock mass parameters. This latter assumption is possible only if the spacing between each inhomogeneity is much smaller than a dominant dimension describing an external geometry of the particular problem. The rock bolt effects are mostly shown as an increase of the rock mass properties, such as elasticity modulus and strength. Improving of the elasticity modulus is mostly done by smearing the bolt elasticity modulus all over the cross section area of the representative volume, with an assumption that strains in the rock mass and the bolt are equal. For increasing of the rock mass strength, so simple an expression is not possible because it is connected with the actual axial force in the bolt and the strength characteristics of the rock mass. The axial force, which is a result of pre-stressing or different deformations along the bolt, causes an additional compression force in the rock mass around the bolt which increases the strength of the rock mass. Wullschläger and Natau (1987) made compression tests on bolted cubes and showed the increase of the strength and the elasticity modulus, but also the breaking strain caused by bolting.

A fully-grouted untensioned bolt in intersection with the joint has a big influence on the joint resistance to shear. The resistance of the bolted joint can be expressed as a sum of the joint and bolt resistances. The bolt resistance was observed in laboratory and in "in situ" tests and it can be divided into two effects: increase of a normal force in the bolt and a "dowel" effect. The increase of the axial tensile force in the bolt caused by relative movements of the joint planes acts in two ways, a component normal to the joint furnishing of an additional shear resistance through a friction effect, and a component parallel to the joint acts as a portion of the joint shear resistance. The "dowel" effect means resistance inducted by shear deformations of the joints, causing penetration of the bolt in the surrounding grout and rock mass. The deformation create shear and bending deformations of the bolt. It is very hard to predict all of these effects because of the highly complicated action which can be seen in Fig. 1. This effect occurs at a slight distance from the joint, and only measures 2–4 diameters of the bolt.

Many have worked on this problem in the last twenty years and their works can be divided into two groups, one which was only concerned with the maximal resistance, and the other which was interested in the behaviour of the bolted joint from the initial state to the failure of the bolt. Most theories from the first group are formed around an axial resistance based only on underformed bolt geometry and around the assumption that the normal force in the bolt is equal to the yield force. Aydan et al. (1987) suggested the formula which included

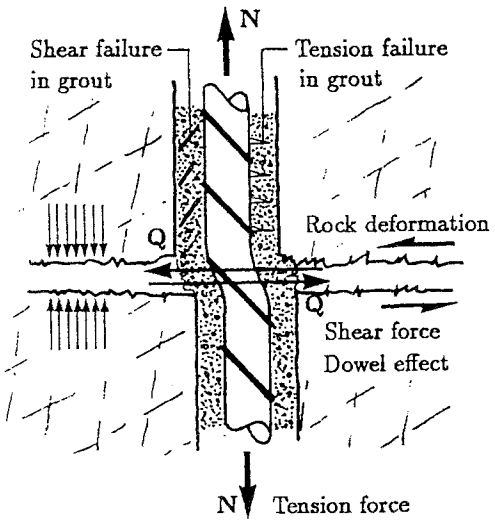

Fig. 1. Action of grouted bolt

the deformed bolt geometry and shear response of bolt. Empirical formulae are used for the "dowel" effect (Bjurström, 1974), which is significant when the bolt is set at a perpendicular angle through the joint. Spang (1988) conducted many shear tests under different conditions and found the relation for the maximal resistance of the bolted joint, which includes most of the important parameters. All these theories consider only the maximal resistance of the bolted joint and do not discuss behaviour before failure.

In order to understand the behaviour of the bolted joint before failure, the complex combined system including the bolt, grout and rock mass around the bolt must be solved. The physical behaviour of this system must be described for shear movement and also for normal movement or for a decoupling of the joint. Panet (1987) suggested that these be calculated as separate problems for which elastic analytical solutions exist. This calculation correlates well with experimental results, but only when the whole system remains elastic, which is only true for very small displacements. From experimental results, Yoshinaka et al. (1988) tried to find a relationship between the displacement at the joint and the bolt resistance. This theory is based on the assumption of the circular deformed bolt shape with some parameters such as statistical values. Brady and Lorig (1988) suggested an element with two springs, one parallel to the local axis of the element and one perpendicular to it. Egger and Pellet (1992), for the purpose of finite element modelling, suggested a representation of the bolted joint by a virtual interface element with equivalent mechanical properties.

In the numerical models, if the rock bolting effect has to be appropriately modelled, the rock bolts have to be represented as special elements. The action of the bolt in the continuous rock mass and near the joint is so different that it is necessary to be modelled as two different elements.

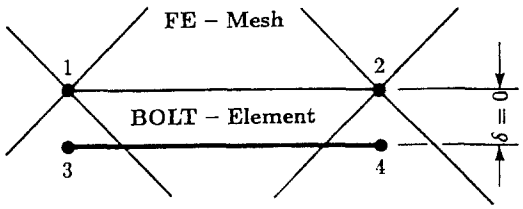

Fig. 2. Four node bolt element and connection with finite element mesh

2. Belt in Continuous Rock Mass

Usually the rock bolts in continuous rock mass are simulated as truss or beam elements (Laabmayr and Swoboda, 1978). These elements are not appropriate to describe rock bolts, especially grouted bolts, because they do not take into consideration the stiffness of the grout. The main disadvantage of the method is that it is not possible to take into consideration different displacements in the bolt and on the surface of the borehole (shear displacement which takes part in grout). To solve this problem some authors have attempted to apply special interface elements between the bolt, represented as one-dimensional elements, and the rock mass. These interface elements were springs in nodes, or special interface elements. Such elements are normally two or three dimensional elements with characteristics of grouted material (Spang, 1988; Siriwardane, 1989), or special joint elements such as the axisymmetrical joint element by Ghaboussi (1973).

A further development of rock bolt elements was an element which included the stiffness of the bolt and the interface. Aydan et al. (1988) developed an element with four nodes, two connected to the rock and two to the bolt. This element can be coupled to regular finite element models with two nodes which represent the grout-rock coupling. The remaining two nodes on the bar are connected with the rock with the stiffness of grout (Fig. 2).

Based on this element a modified rock bolt element (BOLT) was developed. In this model, the nodes on the steel bar and the grout-rock interface have the same coordinates, but the real geometry is based in the stiffness matrix. This stiffness matrix is the sum of the axial stiffness of the bar and the stiffness of the grout annulus. Some assumptions are made for this element:

- the distribution of deformation in longitudinal (local x) direction of the bolt element is linear,
- the distribution of deformation in radial direction, normal to the local axis of the bolt element is constant,
- the distribution of deformation in radial direction in the grout is based on a theoretical analytical solution for axisymmetric bodies. This assumption saves a discretization in the radial direction,
- the normal stress in the longitudinal direction is transferred by the bolt, but in radial direction no stresses are taken into account,
- the shear stress which is the result of a different longitudinal movement in the bolt and on the grout-rock interface is taken by shear resistance of grout,
- the shear stress which is the result of a transversal movement on the grout-rock

interface is taken by the shear resistance of the steel bar. Small transversal movement causes breaking of the grout and loosing of its stiffness,

- the transversal stiffness between the bar and the grout rock interface, "dowel" stiffness, is modelled as an additional spring between the bar and the grout-rock interface nodes in transversal direction.

The bolt stiffness matrix $[K]$ under consideration of expressed assumptions can be written as (1)

where

$$k_b = \frac{E_b A_b}{L}, \quad k_s = \frac{G_b A_b}{L}, \quad k_g = \pi G_g \frac{L}{3\ln(r_h/r_b)}.$$

E_b and G_b are the elasticity modulus and the shear modulus of the bolt, G_g the shear modulus of the grout, A_b the area of the bolt, L the length of the element, r_b and r_h the radius of the bolt and the hole and k_d is the "dowel" stiffness. The "dowel" stiffness is important only on the place where the bolt intersects the rock joint, on which the penetration of bar in the surrounding grout and rock is existing, and it is equal to the shear stiffness of the Bolt Crossing Joint element defined in

$$[K] = \begin{bmatrix} 2k_g & 0 & k_g & 0 & -2k_g & 0 & -k_g & 0 \\ 0 & k_s + k_d & 0 & -k_s & 0 & -k_d & 0 & 0 \\ k_g & 0 & 2k_g & 0 & -k_g & 0 & -2k_g & 0 \\ 0 & -k_s & 0 & k_s + k_d & 0 & 0 & 0 & -k_d \\ -2k_g & 0 & -k_g & 0 & k_b + 2k_g & 0 & -k_b + k_g & 0 \\ 0 & -k_d & 0 & 0 & 0 & k_d & 0 & 0 \\ -k_g & 0 & -2k_g & 0 & -k_b + k_g & 0 & k_b + 2k_g & 0 \\ 0 & 0 & 0 & -k_d & 0 & 0 & 0 & k_d \end{bmatrix} \quad (1)$$

the next section. If the "dowel" is not defined in this way the value can also be calculated from the work of Sydner et al. (1982)

$$k_d = E_b I \left[\frac{E_g}{2E_b I(r_h/r_b - 1)} \right]^{3/4}, \quad (2)$$

where E_g is the elasticity modulus of the grout and I a moment of inertia of the bolt.

Since relatively small displacements of rock can produce very large forces in the bolt, the bolt element should be modelled as an elasto-plastic element. The bolt element consists of two different parts, the bar and the grout, made of different materials, and the post yield definition for both materials have to follow their natural behaviour.

3. Bolt Crossing Joint Element

The behaviour of the rock bolt in intersection with a joint is a very complicated problem for prediction and depends on the characteristics of the joint and many factors connected with the bolt such as: the diameter of the bolt and the hole, the

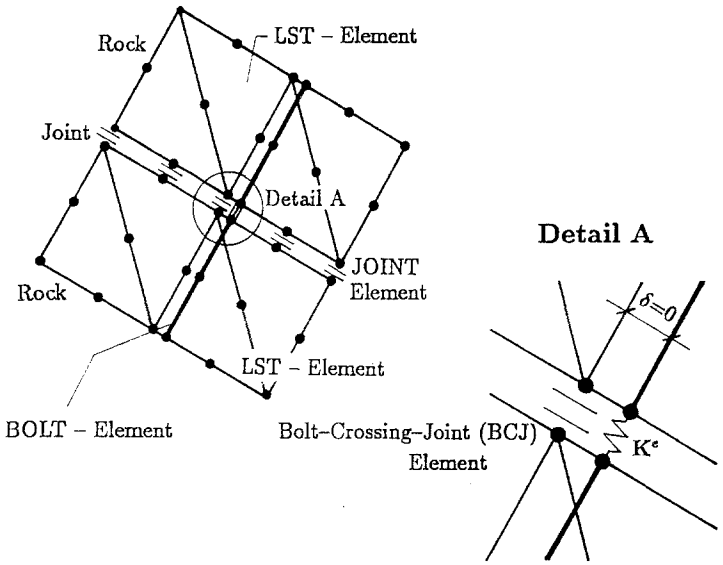

Fig. 3. Bolt crossing joint element and connection with finite element mesh

quality of the steel, the extension of the bolt, the strength of the rock and the grout, and the angle between the joint and the bolt. The rock bolt type also plays an important role. If, at the place where the bolt intersects the joint, a contact between the bar and the surrounding rock does not exist, for example in the case of mechanically anchored or pre-stressed bolts, the bolt acts only with its axial resistance. At the bars which have a continuous contact with the surrounding rock the shear resistance could also mobilised. The grouted bolts, which are the best representation for bolts with continuous connection, could be characterised by the relatively large axial resistance to extension that can be developed over the relatively short bar length and by the high resistance to shear that can be developed by an element penetrating the slipping joint.

A special element, Bolt Crossing Joint (BCJ) element, has been developed to incorporate all important factors. The BCJ element is the element which connects the bolt elements on both sides of the discontinuity (Fig. 3). The BCJ element is assumed to be an element with two nodes, each on one side of the discontinuity, connecting the bar nodes of the bolt element. The other nodes of the bolt element (grout-rock interface) are connected through an interface element representing the joint (Swoboda, 1992).

The BCJ element is modelled as springs which describe the bolt resistance according to the movements on the joint. The stiffness matrix of the bolt crossing joint element can be presented as

$$\mathbf{K}^e = \begin{bmatrix} k_{11} & k_{12} & -k_{11} & -k_{12} \\ k_{21} & k_{22} & -k_{21} & -k_{22} \\ -k_{11} & -k_{12} & k_{11} & k_{12} \\ -k_{21} & -k_{22} & k_{21} & k_{22} \end{bmatrix}, \tag{3}$$

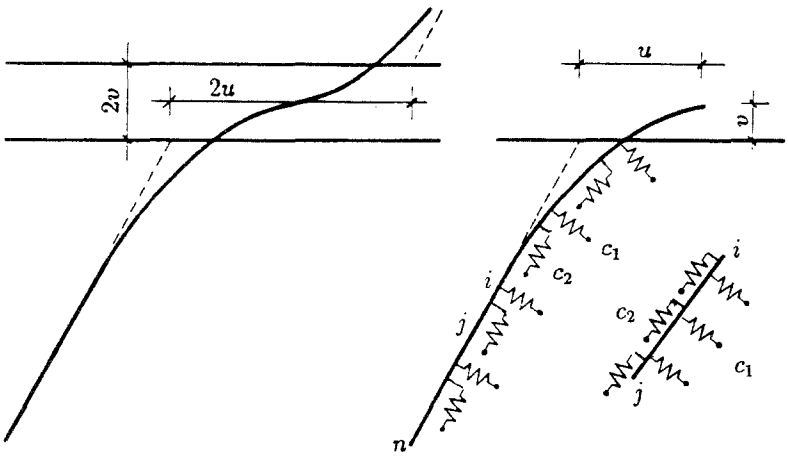

Fig. 4. Substructure system

where k_{11} is a shear stiffness, k_{22} is a normal stiffness, k_{12} represents a connection between a shear displacement and a normal force and k_{21} a connection between a normal displacement and a shear force. The stiffness values depend on a lot of different parameters and explicit expressions are very difficult to prescribe. Here, an additional finite element calculation is suggested for calculating the stiffness matrix components.

The stiffness matrix components are calculated from a substructure (Fig. 4). In this system, with an assumption that the deformation of the bolt is symmetric on both sides of the joint, only the bolt on one side of the joint is taken into account. The bolt near the joint is calculated as a beam structure, with the length which is sufficient to ensure that the support conditions on the side opposite to joint have no influence on results. The beams represent the bar, while the grout and the rock around the bar are modelled as axial and lateral continuously distributed non-linear springs. In this case most of the influences such as the diameter of the bolt and the hole, the quality of the steel, the strength of the rock and of the grout, and the angle between the joint and the bolt can be taken into account. The bolt, before breaking, can take displacement which is in a rank of bolt diameter and the calculation is done based on the theory of large displacements. For the real shear and normal displacement on the joint, a deformed bolt shape and forces in the bolt are calculated. The proposed substructure calculation to find the stiffness matrix components is an iterative procedure.

The substructure stiffness matrix $\mathbf{K}_{\text{sub}}$ is represented as a sum of beam stiffness $\mathbf{K}_b$, spring stiffness $\mathbf{K}_s$ and additional stiffness of the large displacement theory $\mathbf{K}_g$.

$$\mathbf{K}_{\text{sub}} = \sum_{i=1}^{n} \mathbf{k}_b + \mathbf{K}_s + \mathbf{K}_g, \tag{4}$$

where n is the number of the beam elements. The geometry change is taken into account by the way that in every iteration step the system coordinates are changed according to the displacements from the previous step.

The bolt in the intersection with the joint can take large shear and normal displacement before breaking, but plastic deformations of the bar and the surrounding material will occur. The plasticity is included in the substructure calculation according to the direct iteration method. The plastic bar is modelled as a plastic beam element and the grout and the rock are modelled as non-linear lateral and axial springs, with the stiffness dependent on the displacements defined for each substructure element according to actual lateral and longitudinal displacements on element. The solution of the global elasto-plastic substructure problem is done by direct iteration method, which also allows elastic-residual plastic behaviour.

Constitutive Law for Beam

The bar is modelled as a system of beams with normal forces, shear forces and moments in it. The bar material which is mostly steel is modelled as linear elastic-ideal plastic material. The Klöppel-Yamada yield criterion (1958) is used to check if the steel bar is in the plastic condition. This yield criterion F_{Yb} is specially developed for steel beams and it is expressed in forces as

$$F_{Yb} = \frac{M}{M_p} + \left(\frac{N}{N_p}\right)^2 + \frac{16}{3\pi^2}\left(\frac{Q}{Q_p}\right)^2 - 1 = 0. \tag{5}$$

where M, N, Q are the bending moment, normal and shear forces in the bolt and M_p, N_p, Q_p are the plastic forces when only one of these forces is acting.

Lateral Spring Stiffness

The lateral springs describe the grout and the rock stiffness around the bolt in the lateral direction. The stiffness of the spring is defined as a lateral force acting on the bolt divided by a lateral displacement under the bolt. The spring stiffness is not linear and nonlinearity depends on the bolt's lateral displacement. The small lateral displacement produces a big pressure on the grout and rock and for the small displacements plastic deformations in both materials occur.

Based on experiments in which the bar lateral displacements are measured, Prisco et al. (1988) found the experimental formulae for describing the behaviour between the lateral displacement and the lateral stiffness (Fig. 5).

The characteristic values which define the curve were found from experiments for the reinforced bar in the concrete block with a compressive strength of $f_c = 30$ MPa (Prisco et al., 1988). The stiffness values depend on the bar diameter and are based on the different tested diameters ($d_b = 14, 18, 24$ mm). The values are suggested as:

$$k_i = 483.0 - 13.03 d_b \qquad (\mathrm{N/mm^3}) \tag{6}$$

$$k_i = 150.0 - 1.66 d_b \qquad (\mathrm{N/mm^3}) \tag{7}$$

$$v_t = 0.6 \qquad (\mathrm{mm}) \tag{8}$$

$$v_u = 0.316 + 0.302 d_b \qquad (\mathrm{mm}) \tag{9}$$

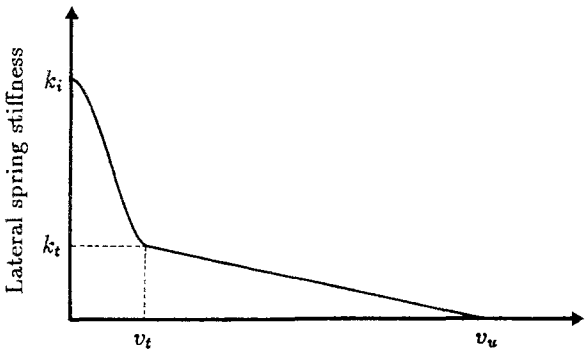

Fig. 5. Lateral displacement – lateral stiffness relationship

From the experiments on the reinforced bar, the shape of the lateral displacement, spring stiffness dependency can be used, but real values on the curve have to be found. The behaviour of the bolt under the lateral displacement is dependent not only on the strength of the grout and the rock mass but also on the bolt and the hole diameter. The real values can be found from a parametric study of the real problem or from the finite element calculation. The experiments and the parametric study for each case are expensive and in most cases impossible. The finite element method can describe the problem well, but the materials have to be modelled very carefully, especially the grout and the rock plastic behaviour. In the region where plasticity occurs the material is fully crashed, which means that the material constants for the crashed material have to be used.

In the substructure calculation the lateral spring stiffness is defined, based on the work of Prisco. The displacement-stiffness function is defined as linear functions on the regions.

Axial Spring Stiffness

The axial spring stiffness describes the behaviour of the bar under the displacement in the direction of the bolt axis. The bar-grout interface plays the main role in this case, because in most cases the slip happened on this plane. Two different stiffness models have to be introduced, dependent on the bolt lateral displacement. If the bolt is moved in the direction of the bolt axis, the real bond-slip relation between the bar and the grout have to be taken into account, and if the bar also has the lateral displacement, the stiffness has to be modelled as a friction between the bar and the crushed grout.

The spring stiffness without the lateral displacement can be defined as a bond stiffness between the bar and the grout. The spring stiffness c_2 is then defined as the bond force divided by the corresponding slip displacement s (Fig. 6),

$$c_2 = \frac{\tau d_b \pi}{s} \tag{10}$$

where τ is a maximal bond stress for the applied slip s, and d_b is the bolt diameter.

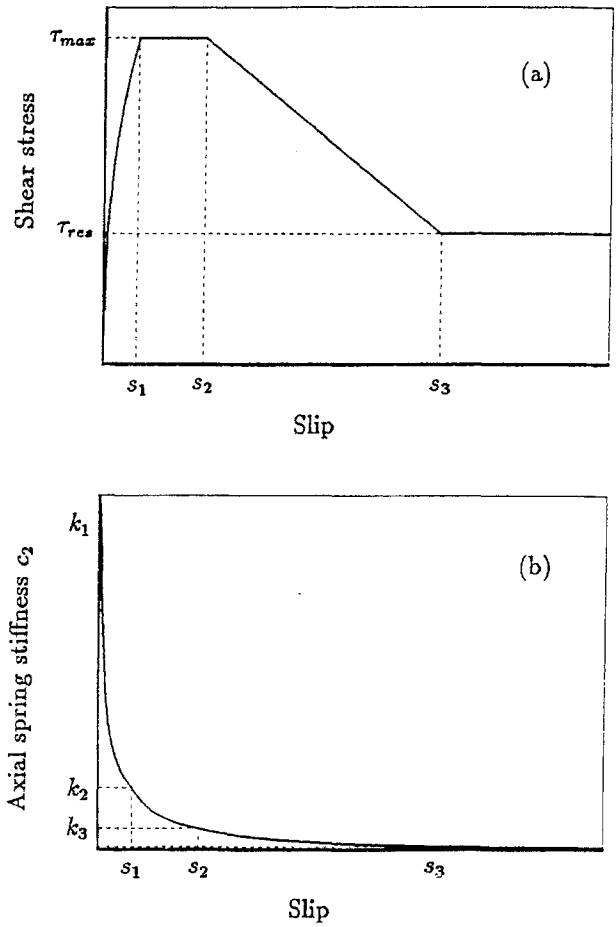

Fig. 6. Bond-slip relationship (**a**) and calculated stiffness-slip relationship (**b**)

This relationship between the bond force and the slip can be found from the experiments or can be taken as suggested values from the CEB-FIP model code for 1990. The Code suggested the bond-slip relationship based on the concrete compressive strength to be different for a ribbed and for a smooth bar.

If the lateral displacement of the bar exists, the bond between the bar and the grout is destroyed and only a friction between the bar and the crushed zone is active. This can happen only when a certain lateral displacement takes place, which produces a debonding between the bar and the grout on the one side and the plastic deformations of the grout on the other side of the bar. For the lateral displacement which produces this effect, a value the same as the height of the ribs can be taken. If the displacement is bigger than this limit, the maximal axial force can be defined as a product of the active lateral force and the friction coefficient.

Convergence Process

The substructure calculation is a non-linear iterative procedure. The convergence

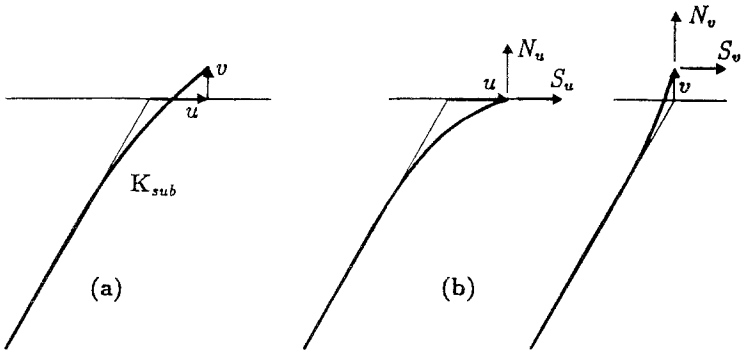

Fig. 7. Definition of the substructure system stiffness matrix (**a**) and calculation of the BCJ stiffness matrix terms (**b**)

of the process is checked by two criteria; the displacements and the plasticity of the bar.

The displacement criterion checks that the difference between the displacements in two adjoining calculations is smaller than the allowed tolerance. The displacement check is important for the large displacement theory and also for the selection of the right spring stiffness. This check is done for all nodes in the axial and the lateral direction. The plasticity criterion verifies if the stresses in each part of the bar are smaller than the yield stress. This criterion is checked only if the displacement criterion is satisfied. When both criteria are satisfied, the stiffness of the substructure system is found and the BCJ element stiffness matrix components can be found.

For the verification of the substructure calculation specially prepared samples are indispensable. The substructure calculation verification is made on two separate examples; one for lateral and one for axial displacement, for which the experimental data exist. The calculated results concur satisfactorily with experimental results (Marenče, 1992).

Definition of BCJ Stiffness Matrix Components

The stiffness of the bolt in the intersection with the joint is very sensitive according to the size and the combination of the shear and the normal displacement which takes part on the joint. Due to this fact, the stiffness of the substructure system is defined for the real displacements on the joint, u, v found in the previous iteration step of the total system (Fig. 7). Application of the separate displacement on the substructure with defined stiffness, a normal and a shear force in the bolt can be detected and from this terms of the BCJ element stiffness matrix defined in Eq. (3).

Application of the shear displacement u on the substructure a shear force S_u and a normal force N_u in the bar is found, and the stiffness terms defined by the shear displacement are

$$k_{11} = \frac{S_u}{2u} \tag{11}$$

$$k_{12} = \frac{N_u}{2u}, \tag{12}$$

In the substructure calculation only half of the system is calculated and the BCJ elements stiffness has to be defined for a total joint displacement. On analogy, applying of the normal displacement v a shear force S_v and a normal force N_v in the bar is found and the stiffness terms are defined as

$$k_{21} = \frac{S_v}{2v} \tag{13}$$

$$k_{22} = \frac{N_v}{2v}. \tag{14}$$

The stiffness matrix of BCJ element defined in this way is not symmetric because the terms k_{12} and k_{21} are not equal. Non-symmetry is very small and symmetrization in the form

$$k_{12}^* = \frac{k_{12} + k_{21}}{2} \tag{15}$$

can be used. Equation (3) which defines the BCJ stiffness matrix is modified in the equation

$$\mathbf{K}^e = \begin{bmatrix} k_{11} & k_{12}^* & -k_{11} & -k_{12}^* \\ k_{12}^* & k_{22} & -k_{12}^* & -k_{22} \\ -k_{11} & -k_{12}^* & k_{11} & k_{12}^* \\ -k_{12}^* & -k_{22} & k_{12}^* & k_{22} \end{bmatrix}. \tag{16}$$

The components of the stiffness matrix are sensitive according to the shear and the normal displacement.

4. Shear Experimental

By means of simple laboratory tests, such as pull-out and shear tests, the required parameters for bolt description in the finite element calculation can be found or their selection can be confirmed. To prove the rock bolt model, pull-out and shear tests for different bolt types have been done. (Swoboda et al., 1992; Marenče, 1992). Here, results of shear tests with grouted bolts are show.

In the laboratory shear tests, concrete blocks were connected by grouted bolt, set perpendicular to the joint. The bolt, a ribbed steel bar with 26 mm diameter, was installed according to regular procedures in tunnelling. To reduce the joint influence, tests have been done with Teflon plates between blocks and without normal pressure on the joint. The shear force resulting from the (app. monotonous) shear displacement was measured. Based on the presented theory, the laboratory shear test was numerically modelled and results are compared. The selection of the parameters, important for BCJ definition, are proved. The longitudinal spring stiffness definition, based on the bond between steel and grout, has been checked by a pull-out test and concur well with the values defined by the

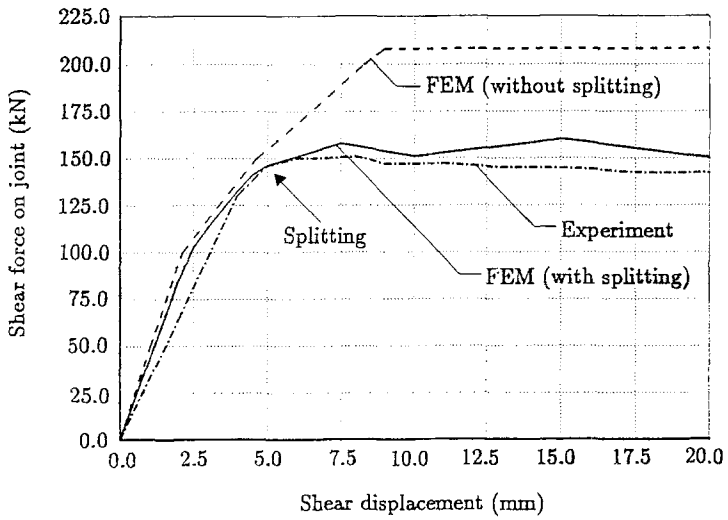

Fig. 8. Measured and calculated shear force–shear displacement behaviour

CEB-FIB code (1990), for the ribbed bar (Marenče, 1992). The lateral spring stiffness has been defined by the work of Prisco et al. (1988). The shear force – shear displacement diagram is shown in Fig. 8. The numerical results concurred satisfactorily with the experiments until the applied force reached 150 kN. At that point in the experiment the sheared block split under the bolt. The changing of the lateral spring stiffness definition in the substructuring calculation of the BCJ element and the splitting of the block can be also modelled.

5. Behaviour of the Bolted Joint

Based on the performed laboratory tests, the necessity input data for the finite element calculation was proved and the influence of different parameters on the shear resistance of bolted joint, such as a bolt setting angle, joint strength parameters, or a joint dilatancy angle, is then studied. The study was made on the numerical simulation of the standard direct shear test.

Influence of Bolt Setting Angle

The setting angle is one of the most important parameters which influence the behaviour of the bolted joint. Figure 9a shows the influence of the bolt setting angle on a mobilised shear force as a function of shear displacement for selected setting angles. The results are compared with different theories presented in the literature on the subject. The results obtained correlate well with the work of Bjurström (1974) and Aydan (1987) except when the setting angle is approximately 90°. This is because all these theories only give consideration to the effect of the normal force and not to that of the "dowel" effect. The expression defined by Spang (1988) took both effects into consideration because it has been derived as an

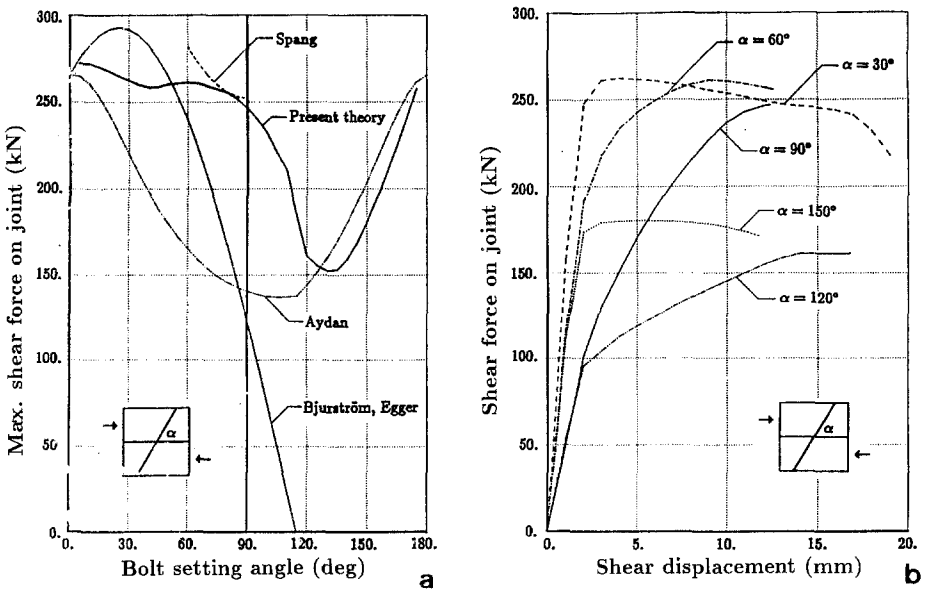

Fig. 9. Influence of bolt setting angle

empirical formula from many shear tests. This equation is only valid for setting angles between 60° and 90° and correlates well in this range with the present theory. Figure 9b shows the maximal resistance of a bolted joint for the whole range of setting angles.

Influence of Joint Strength Parameters

The joint strength is usually represented by the linear Mohr-Coulomb strength law. In this presentation the joint strength is expressed in terms of a cohesion and a friction angle. Additional normal pressure on the joint caused by shearing of the bolt, together with the joint friction, produces supplementary shear resistance of the bolted joint. The effect of different friction angles on the maximal resistance of the bolted joint is shown in Fig. 10a. Increase of the maximal resistance for the setting angles until 110° is obvious. For setting angles over 110° shearing causes a compression force in the bolt, which decreases the normal pressure on the joint and thereby the additional resistance of the bolted joint.

If the bolt, as a special element, is not included in the numerical calculation, the resistance parameters which define the joint resistance can be increased. Numerical shear tests with and without the bolt have been performed. For both cases, the normal pressure on the joint has been varied. The results, show in Fig. 10b, show that the effect of rock bolting on joint shear resistance can be described as an increase in joint cohesion without a change in the friction angle, also found from experimental results (Bjurström, 1974; Wullschläger et al., 1987). The increase in cohesion can be expressed as the additional joint shear resistance caused by the bolt divided by the joint area corresponding to one bolt.

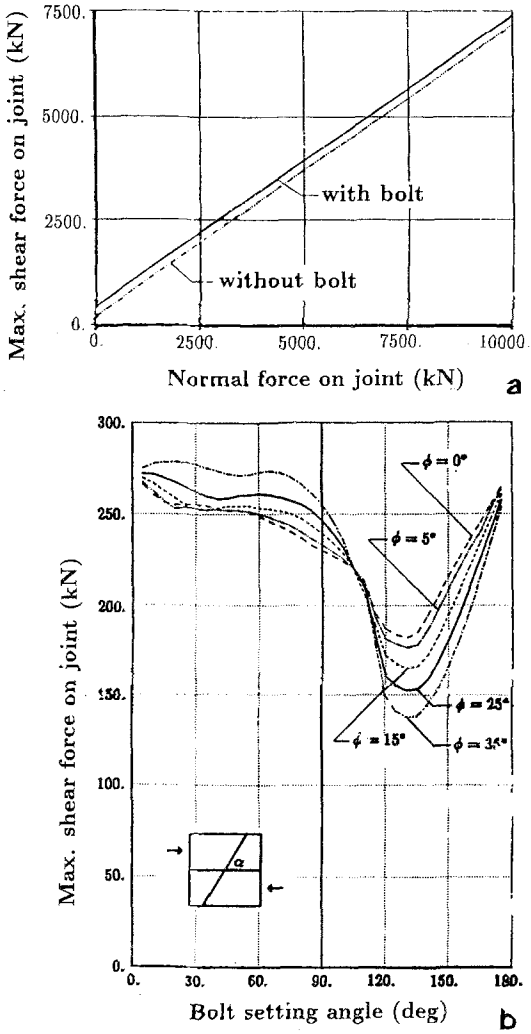

Fig. 10. Influence of joint strength parameters

Influence of Joint Dilatancy

Dilatancy describes the normal displacement (joint thickening) caused by shear. In the numerical calculation it is conventionally approximated by a dilatancy angle i, defined as

$$i = \arctan\left(\frac{\Delta v}{\Delta u}\right), \tag{17}$$

where Δv is a normal displacement caused by a shear displacement Δu on the joint. The joint thickening induces a larger normal force on the joint, and through joint friction, increases the resistance of the bolted joint. Also, the joint thickening

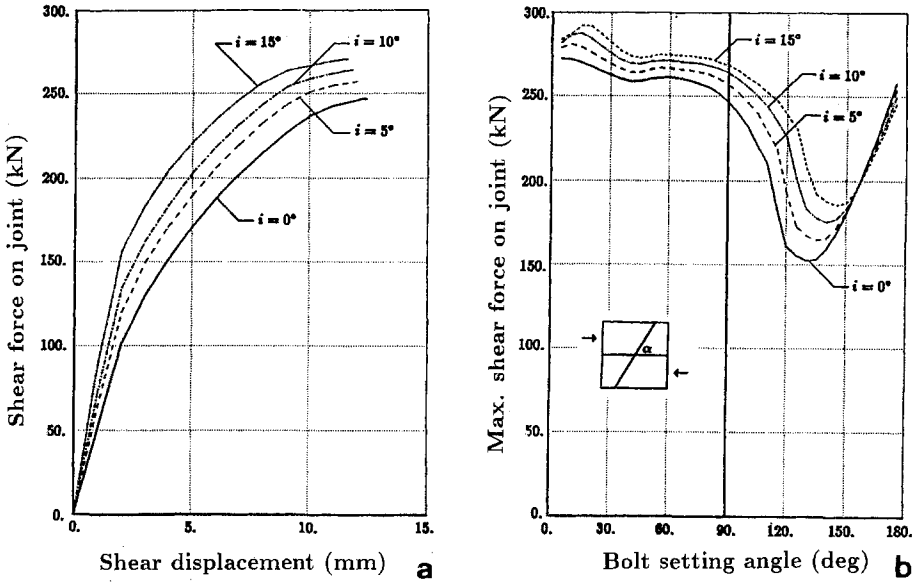

Fig. 11. Influence of joint dilatancy

induces a larger bolt strain and causes breaking of the bolt at a smaller shear displacement. Results of numerical shear tests, with different dilatancy angles, for the bolt set perpendicular to the joint, are shown in Fig. 11a. Figure 11b shows the maximal resistance of a bolted joint for the whole range of setting angles for the different dilatation angles. The increase of the maximal shear resistance is obvious.

Table 1. Material parameters

Rock			
E	130.00	MN/m^2	Elasticity modulus
ν	0.38	–	Poisson's ratio
γ	25.00	kN/m^3	Unit weight
c	120.00	kN/m^2	Cohesion
c_r	80.00	kN/m^2	Cohesion at rest
ϕ	22.00	deg	Friction angle
ϕ_r	18.00	deg	Friction angle at rest
Shotcrete modulus of elasticity			
E_1	5000.00	MN/m^2	Young shotcrete
E_2	20000.00	MN/m^2	Old shotcrete
Rock bolts			
d_b	26.00	mm	Bolt diameter
d_h	40.00	mm	Hole diameter
σ_y^b	500.00	MN/m^2	Bolt yield stress
τ_{max}^g	14.00	MN/m^2	Peak bond strength
τ_{res}^g	5.00	MN/m^2	Residual bond strength

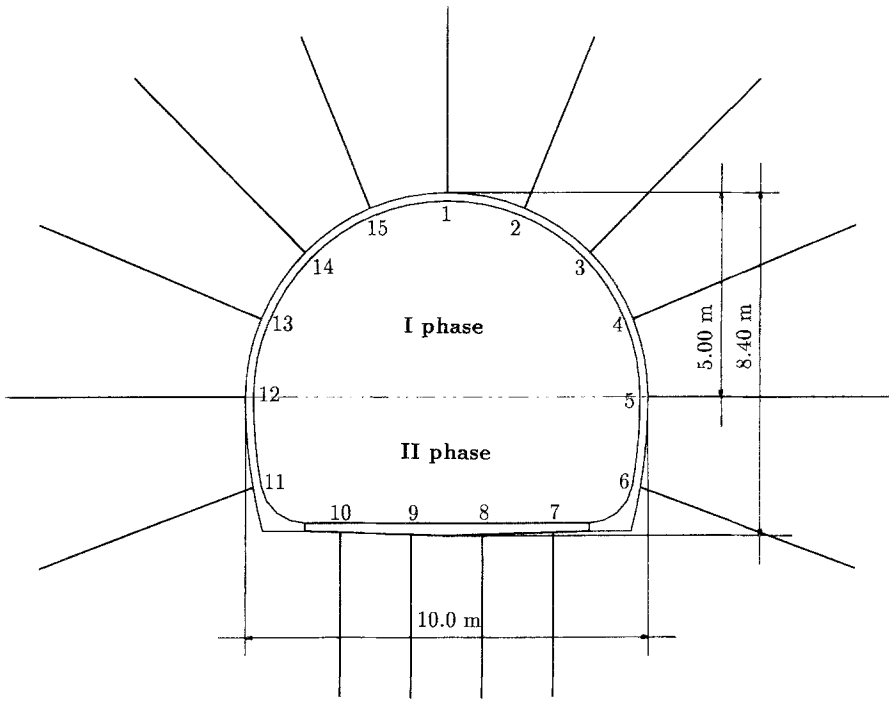

Fig. 12. Geometry of the tunnel

6. Illustrative Example

Implementation of rock bolts in the numerical model which simulates excavation and stabilsation of an underground opening is demonstrated on one road tunnel in Australia. The tunnel is excavated under difficult geological conditions in a moraine with a maximal overburden of 70.0 m. Rock parameters and parameters defining the supporting system, consisting of shotcrete lining and rock bolts, are shown in Table 1.

The rock mass is modelled by linear strain triangular elements as a homogeneous isotropic elasto-plastic material. The plastic behaviour is defined by the Mohr-Coulomb failure criteria with peak and residual strength parameters. The shotcrete lining is modelled as beam elements. Development of shotcrete stiffness with time is, in the calculation, expressed by a modulus of elasticity dependent on shotcrete age. Grouted bolts are modelled as BOLT elements. The length of the bolts is between 4.5 and 6.0 m. The geometry of the tunnel and the position of the bolts is shown in Fig. 12.

The initial state of stress is assumed from the geological conditions. The vertical initial state of stress is taken as a linear distribution in depth with an overburden of 70 m. The horizontal initial state of stress is taken as a portion of vertical stress with a coefficient of horizontal stress of 0.6. The three-dimensional effect of excavation is taken into account by initial stress relief before excavation. In this

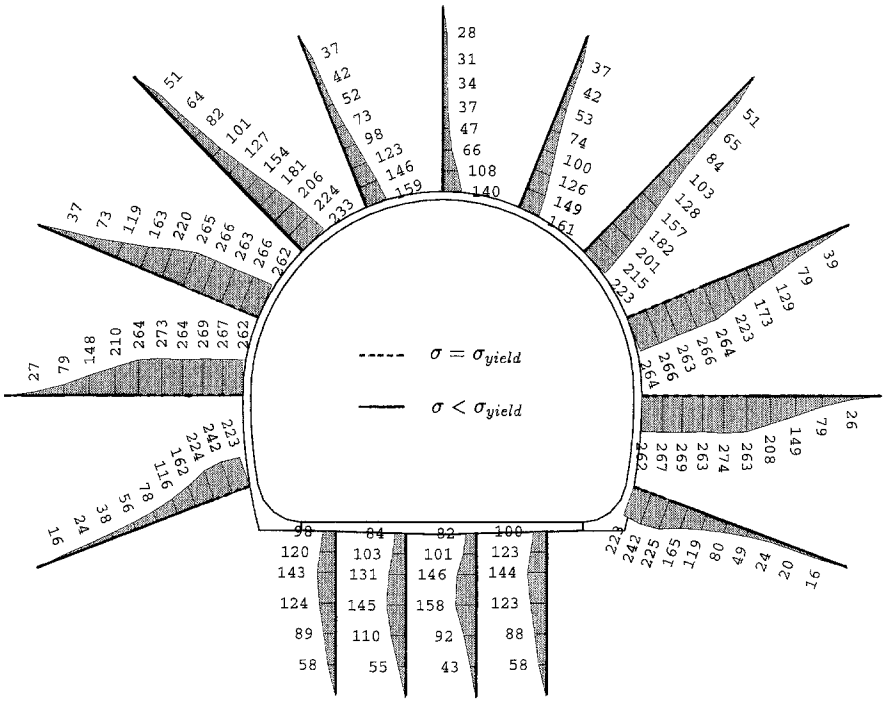

Fig. 13. Axial force in bolts for final loading step

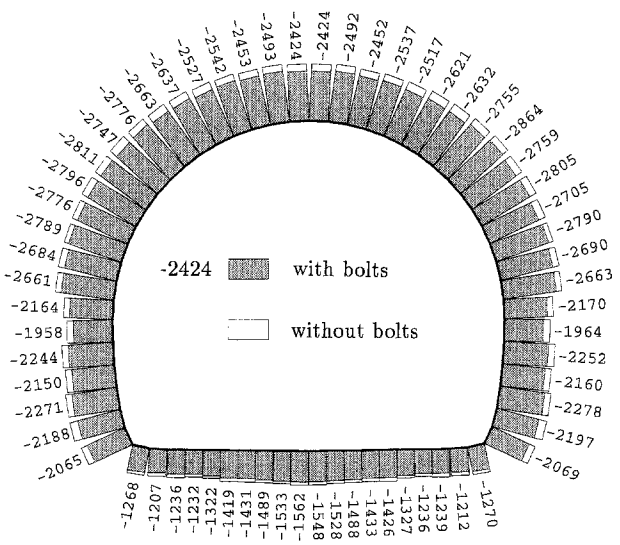

Fig. 14. Axial forces in lining for the calculation with and without rock bolts

way, displacements taking place before excavation are included in the calculation. The factor defining initial stress relief α is 0.3 (Swoboda, 1989).

Excavation of the tunnel was undertaken in two steps, a crown and then a bench. The loading steps follow the excavation phases, with indispensable partition. After finishing excavation and lining installation of the crown, the plastic calculation is performed to partly release the over-stressed rock regions. At the end, all over-stressed rock regions are released.

Some representative results, for the final situation, are shown here. Distribution of axial force in the bolts is shown in Fig. 13. It can be seen that the part of the bolts 4–6 and 11–14 are plastified after the last construction stage, due to very bad rock conditions. In contrast to these high loaded bolts, the bolts in the crown are not fully loaded, but their role is also to prevent possibly instable rock blocks from falling. The bolts at the bench also bear a small force compared at the yielding force of a bolt. The importance of these bolts is to reduce the bending moments in the concrete beam caused by plastic deformations under the tunnel.

The effect of rock bolts on the normal force in the shotcrete lining is shown in Fig. 14. Installed bolts reduce the lining deformations and thus normal forces in lining, but the rock bolts also exert internal pressure on the lining.

7. Conclusions

Rock bolts represent a very efficient method of increasing rock mass strength. The effect of rock bolts is very well known from engineering practice and laboratory tests, but it is difficult to quantify it. For the influence of rock bolts on rock mass, one must distinguish between the behaviour in intact rock mass and the behaviour when a bolt passes through rock fault or discontinuity. The behaviour is so different that two different finite elements are proposed for description of bolt behaviour; one in the intact rock mass and one when the bolt intersects the fault system.

In the intact rock mass a bolt acts as an increase in rock mass stiffness and strength, particularly tension and shear strength. Bolt action in intact rock mass can be easily modelled by BOLT elements which give satisfactory results compared with an analytical solution. Behaviour of a bolt in intersection with a fault can be divided into two effects: the increase of axial tensile force in a bolt and a "dowel" effect. The behaviour of a bolt in intersection with a fault is complicated to analyse being influenced by many parameters such as: the shape and type of bolt, the diameter of the bolt and the hole, the steel quality, the angle between the joint and the bolt, the strength of the grout and the rock and the characteristics of fault as a strength and dilatancy. Predicting all parameters having an influence on the resistance of a bolted joint is very difficult using one expression, which is why a small finite element calculation is suggested here. In the calculation, the real forces and the bolt stiffness are found for the real shear and normal movement on a joint.

Numerical modelling of simple laboratory tests, such as pull-out and shear tests concur satisfactorily with experimental results. On the basis of experiments, the behaviour of a bolted joint, defined for specific conditions, can be extended to

other cases. A few simple tests combined with inexpensive numerical calculations, can be an easy and inexpensive means of defining the bolted joint behaviour for all parameters of interest. In this way, the effect of an existing bolt type can be proved or a new bolt type can be tested or developed.

Elements describing the behaviour of the bolt are defined for a grouted bolt, as the most commonly used bolt type, but can be used with simple modification for other bolt types.

Acknowledgements

The authors express their gratitude to the "Jubiläumsfond der Österreichischen Nationalbank" for promoting this research project (No. 4793 and 4800) and to the "Forschungsförderungsfond der gewerblichen Wirtschaft" – Project RD-Anker, which made it possible to conduct essential fundamental investigations on the impact of rock bolts in the New Austrian Tunnelling Method. The authors wish to acknowledge with thanks the company Mayreder Consult, Linz, Austria, for the performance of most experiments.

References

Aydan, Ö., Kyoya, T., Ichikawa, Y., Kawamoto, T., Ito, T., Shimizu, Y. (1988): Three-dimensional simulation of an advancing tunnel supported with forepoles, shotcrete, steel ribs and rockbolts. In: Swoboda (ed.), Numerical methods in geomechancis, Balkema, Rotterdam, 1481–1486.

Aydan, Ö., Kyoya, T., Ichikawa, Y., Kawamoto, T. (1987): Reinforcement effects of rockbolts and their analysis. In: Proc., 22nd Japan National Conference on Soil Mechanics and Foundation Engineering, Niigata, Japan, 923–926.

Bjurström, S. (1974): Shear strength of hard rock joints reinforced by grouted untensioned bolts. In: Proc., 3rd Congress of the ISRM, Denver, 1194–1199.

Brady B., Lorig, L. (1988): Analysis of rock reinforcement using finite difference methods. Computers and Geotechnics 5, 123–149.

CEB-FIP Model Code 1990, Final Draft (1991): Bulletin D'Information No. 203, Chapter 3.

Egger P., Pellet F. (1992): Numerical and experimental investigation of the behaviour of reinforced jointed media. In: Proc., Fractured and Jointed Rock Masses, Lake Tahoe, California, 277–282.

Ghaboussi, J., Wilson, E. L., Isenberg, J. (1973): Finite element for rock joints and interfaces. ASCE, J. Soil Mech. Found. Div. 99 (SM10), 833–848.

Klöppel, K., Yamada, M. (1958): Fließpolyester des Rechteck- und I-Querschnittes unter der Wirkung von Biegemoment, Normalkraft und Querkraft. Stahlbau 27, 284–290.

Laabmayr, F., Swoboda, G. (1978): The importance of shotcrete as support element of the NATM. In: Proc., 2nd Shotcret Conference, Eng. Foundation, St. Anton, 65–79.

Marenče, M. (1992): Numerical model for rockbolts under consideration of rock joint movements. Doctorate Thesis, Innsbruck University, Austria.

Panet, M. (1987): Reinforcement of rock foundations and slopes by active or passive anchors. In: Proc., 6th Int. Congress ISRM, Montreal, 1411–1420.

Pellet, F. (1994): Strength and deformability of jointed rock masses reinforced by rock bolts. Dissertation No. 1169, Ecole Polytechnique Federal de Lausanne, Switzerland.

Prisco, di M., Ottanà, S., Sesana, S. (1988): Modellazione non lineare dell'azione di spinotto di una barra immersa in una massa illimitata di calcestruzzo. Studi e ricerche, corso di perfezionamento per la construzioni in cemento, Vol. 10. Politecnico di Milano, Italia.

Siriwardane, H. J. (1989): Numerical analysis of anchors in soil – Application brief. Int. J. Numer. Analyt. Meth. Geomech. 13, 427–433.

Spang, K. (1988): Beitrag zur rechnerischen Berücksichtigung vollvermörtelter Anker bei der Sicherung von Felsbauwerken in geschichtetem oder geklüftetem Gebirge. Doctorate Thesis, Lausanne University, Switzerland.

Swoboda G. (1989): Numerical modelling of tunnels. Numerical methods and constitutive modelling in geomechanics, CISM Courses and Lectures No. 311, Udine, 277–318.

Swoboda, G. (1992): Programmsystem FINAL – Finite Element Analyse linearer und nichtlinearer Strukturen unter statischer und dynamischer Belastung, Version 6.6, Universität Innsbruck, Austria.

Swoboda, G., Marenče, M., Ertan, H. (1992): Rock anchors in jointed rock. 2nd Czechoslovak Conference on Numerical Methods in Geomechanics, Prague, Czechoslovakia, 116–127.

Sydner, V. W., Schwab, P. M., Gerdeen, J. C. (1982): An elastic solution for the shear stiffness of the fully grouted resin roofbolt. In: Proc., Int. Symp. on Strata Mechanics, Newcastle upon Tyne, 237–240.

Wullschläger D., Natau O. (1987): The bolted rock mass as an anisotropic continuum – Material behaviour and design suggestion for rock cavities. In: Proc. 6th Congress Int. Soc. Rock Mech., Montreal, 1321–1324.

Yoshinaka R., Shimizu T., Arai H., Ariska S. (1988): Experimental study on the rock bolt reinforcement in jointed rock mass. Romana (ed.) Rock mechanics and power plants, Balkema, Rotterdam, 427–435.

Authors' address: Dr. Miroslav Marenče, Geomechatronic Center Linz, Hauptstrasse 99, A-4232 Hagenberg i.M., Austria. Prof. Dr. Gunter Swoboda, Department of Numerical Methods in Structural Engineering, Innsbruck University, Technikerstrasse 13, A-6020 Innsbruck, Austria.